·综述· ·明日之星专栏·

基于开环反应构建高性能可降解阳离子聚合物及其生物应用

赵亚琪 孙玉洁 俞丙然* 徐福建*

(北京化工大学材料科学与工程学院 北京 100029)

摘 要 不可降解的阳离子聚合物会在体内累积，会对人类健康造成潜在危害，限制了阳离子聚合物的应用. 因此，开发生物相容性高、可降解性能好的阳离子聚合物材料具有重要意义. 开环反应是获得可降解阳离子聚合物的方法之一，使阳离子聚合物具有更好的可降解性能及生物安全性. 本文主要介绍了3种基于开环反应的可降解阳离子聚合物的构建策略，包括“一锅法”多胺基多环氧的开环反应、*N*-羧基环内酸酐(NCA)开环聚合和双硫交换反应，不同的构建策略制备出具有独特结构的可降解阳离子聚合物，包括支化阳离子聚合物、多肽阳离子聚合物、聚二硫化物，不同的结构赋予了可降解阳离子聚合物更高的性能. 此外，对高性能可降解阳离子聚合物在核酸递送、抗菌等方面的生物应用进行了总结.

关键词 阳离子聚合物，开环反应，可降解，递送载体，抗菌材料

引用: 赵亚琪, 孙玉洁, 俞丙然, 徐福建. 基于开环反应构建高性能可降解阳离子聚合物及其生物应用. 高分子学报, **2025**, 56(2), 200−214

Citation: Zhao, Y. Q.; Sun, Y. J.; Yu, B. R.; Xu, F. J. High-performance degradable cationic polymers based on ring-opening reactions and their biological applications. *Acta Polymerica Sinica*, **2025**, 56(2), 200−214

阳离子聚合物是结构中带有正离子的聚合物，因其独特的正电特性，而备受关注. 阳离子聚合物通过来源分类可分为天然衍生的阳离子聚合物和人工合成的阳离子聚合物，并以人工合成为主. 常见的人工合成的阳离子聚合物有聚乙酰亚胺类阳离子聚合物[1~3]、聚碳酸酯阳离子聚合物[4~6]、丙烯酸衍生物[7~9]等， 可以通过设计结构、后期修饰等方法赋予聚合物更多功能，从而实现更好的生物学性能. 此外，天然多糖富含羟基基团，在阳离子聚合物上引入多糖可以延长阳离子聚合物在体内循环时间，提高材料生物相容性，是十分有潜力的生物医用材料[10~12]. 近年来，阳离子聚合物在基因治疗[13,14]、药物递送[15,16]、抗菌[17,18]等领域有较为广泛的应用. 在基因治疗方面[19]，基因载体对于治疗基因的导入至关重要，载体作为治疗基因的“运载工具”，帮助其进入目标细胞或组织中并完成释放，因此制备有效的递送载体是基因治疗的核心问题之一. 阳离子聚合物是非病毒基因递送载体的一个主要类型，可以通过静电作用同治疗基因结合，形成带有正电性的复合物，协助治疗基因通过细胞膜进入细胞，释放核酸，实现有效递送. 在药物递送方面[20]，阳离子聚合物可以通过化学键修饰、自组装、静电相互作用等多种方式负载药物，递送其进入靶细胞，发挥药物的功能以达到治疗疾病的效果. 在抗菌方面[21]，阳离子聚合物可以通过静电作用与带负电的细菌或真菌细胞膜发生强相互作用，扰动并破坏细胞膜进而杀死细菌或真菌，因此在抗菌方面备受关注.

生物应用的阳离子聚合物材料需要可降解性能，然而常见的阳离子聚合物制备方法，如原子转移自由基聚合[22]、可逆加成断裂链转移聚合[23]、迈克尔加成反应[24]等，存在聚合物主体的C−C键主链不可完全降解、易发生副反应等

2024-09-18收稿，2024-10-24录用，2025-01-10网络出版；国家自然科学基金(基金号 22122501，22475015)资助.

* 通信联系人，E-mail: yubr@mail.buct.edu.cn; xufj@mail.buct.edu.cn

doi: 10.11777/j.issn1000-3304.2024.24242; CSTR: 32057.14.GFZXB.2024.7318

问题，难以满足需求，因而需要研究探索新的构建方法，以扩展阳离子聚合物在生物领域的应用范围. 可降解生物材料在体内环境中能够因分子链发生特异性或非特异性断裂而逐步降解，且降解产物可以被人体吸收或经代谢过程排出体外，不会对人类健康造成伤害，近年来成为研究的重点方向. 自由基开环聚合[25]、多胺基-多环氧开环聚合[26]、*N*-羧基环内酸酐(NCA)开环聚合[27]、氨基酸-*N*-硫代羧酸酐(NTA)开环聚合[28]、*N*-苯氧羰基氨基酸(NPC) 开环聚合[29]、双硫交换聚合[30]等方法均可构建可降解阳离子聚合物. 其中，自由基开环聚合单体选择性多，增加了聚合物材料的多样性，然而，自由基开环聚合具有单体合成烦琐、难均聚等问题，仍需研究者不断突破[25]；NTA开环聚合对制备、存储、聚合环境条件要求低，是制备功能化聚氨基酸的方法之一，但NTA聚合速率较慢，可用引发剂种类较少，仍需进一步研究；NPC开环聚合单体具有较好的稳定性，聚合对水、醇的耐受性良好，且高温下聚合效率高，是一种可靠的聚氨基酸合成方法，但NPC开环聚合在室温下聚合速率低，副产物较多，聚合机理不明确，需进一步改进[31]. 多胺基-多环氧开环聚合、NCA开环聚合和双硫交换聚合操作简单、条件温和，聚合产物结构灵活、易于改性，被广泛开发用于可降解阳离子聚合物的制备.

本文着重介绍了3种构建高性能可降解阳离子聚合物的方法——“一锅法”多胺基多环氧的开环反应、NCA开环聚合和双硫交换反应构建高性能可降解阳离子聚合物，以及高性能可降解阳离子聚合物在核酸递送、抗菌、药物递送等领域的应用.

1　“一锅法”多胺基-多环氧开环反应构建策略

受迈克尔加成反应的启发，徐福建课题组以多胺基/多环氧化合物为出发点，通过“一锅法”开环反应合成了系列支化阳离子聚合物. 多胺基-多环氧开环反应是一种简单的化学转化，2种或多种含有胺基或环氧基团的多官能团结构单元可以通过分步生长来制备阳离子聚合物[32,33]. 胺基基团中的氮原子带有孤对电子，可以作为亲核试剂攻击环氧化合物使得环氧基团裂解，同时形成二级胺基和羟基，为后续反应提供了大量活性位点，在实现快速聚合的同时也实现了聚合物的支化. 支化阳离子聚合物具有支化的三维树枝状结构，分子内具有较多空腔，可以有效络合核酸并且保护其不受各种生物分子的影响；支化阳离子聚合物结构灵活，易于修饰，可以按需引入各类功能基团，提高相关性能[34]. 此外，“一锅法”多胺基-多环氧开环反应可以通过向反应单体中引入二硫键、正交酯基团等响应基团，制备出可降解支化阳离子聚合物，当可降解支化阳离子聚合物接收到刺激信号 (如谷胱甘肽、pH等)时响应基团断裂，聚合物发生降解，促进核酸的释放，提高转染效率[35] (图1(a)).

基于“一锅法”多胺基-多环氧制备策略，研究者们构建出多种可降解的支化阳离子聚合物，简易的合成方法、优异的生物性能让可降解支化阳离子聚合物在生物材料领域的应用具有十分重要的意义，成为非常有前景的核酸递送载体以及抗菌材料. 如图1(b)所示，Qi等[36]通过邻位酯二胺和异氰尿酸三缩水甘油酯(TGIC)开环聚合，并加入过量的乙二胺封端，合成了酸响应性聚合物(ARP)，随后通过胺基环氧开环反应将氟化烷基链装饰到ARP上，生成了新型氟化酸响应性支链富羟基阳离子(ARP-F). ARP-F具有良好的pH响应降解性和生物相容性，可有效负载pCas9-surv质粒并联合替莫唑胺通过增加癌细胞对抗癌药物的敏感性，进一步增强肿瘤抑制活性(图1(c)和1(d)). 如图1(e)所示，Ye等[37]先使用胱胺和D-赖氨酸的酰胺化反应合成了二硫键修饰的赖氨酸单体(SK)，再将SK与TGIC进行开环聚合获得新型还原响应性降解的支化核酸载体(SKP). 将SKP搭载血管内皮生长因子质粒(pVEGF)后涂敷在血管支架上，植入兔主动脉中观察性能. 结果表明，通过在血管支架上涂敷该基因载体复合物能在初期实现VEGF的过度表达，进而促进再内皮化的进程，最终缓解支架内再狭窄的情况(图1(f)~1(h)). 如图1(i)所示，Qi等[38]先以*β*-乳糖和光胺为原料制备了氨基修饰的乳糖，再同TGIC开环反应制备了具有还原响应性的支化阳离子基因载体(LBP). LBP具有良好的还原反应降解性、生物相容性，可有效递送

pCas9-survivn质粒，引入的乳糖可以同肝细胞癌细胞表面高度表达的Asialal糖蛋白受体特异性结合，用于治疗原位肝细胞癌(图1(j)和1(k)).

如图2(a)所示，Huang等[26]通过“一锅法”多胺基-多环氧的开环反应，将羟乙基二硫二缩水甘油醚与庆大霉素、妥布霉素、新霉素开环反应，合成了一系列胺基糖苷类阳离子聚合物还原型HP (SS-HP). Xiao等[39]的研究表明SS-HPT除了具有优异的抗菌效果外，还可以有效清除受伤后的细胞游离核酸，从而抑制损伤相关分子模式

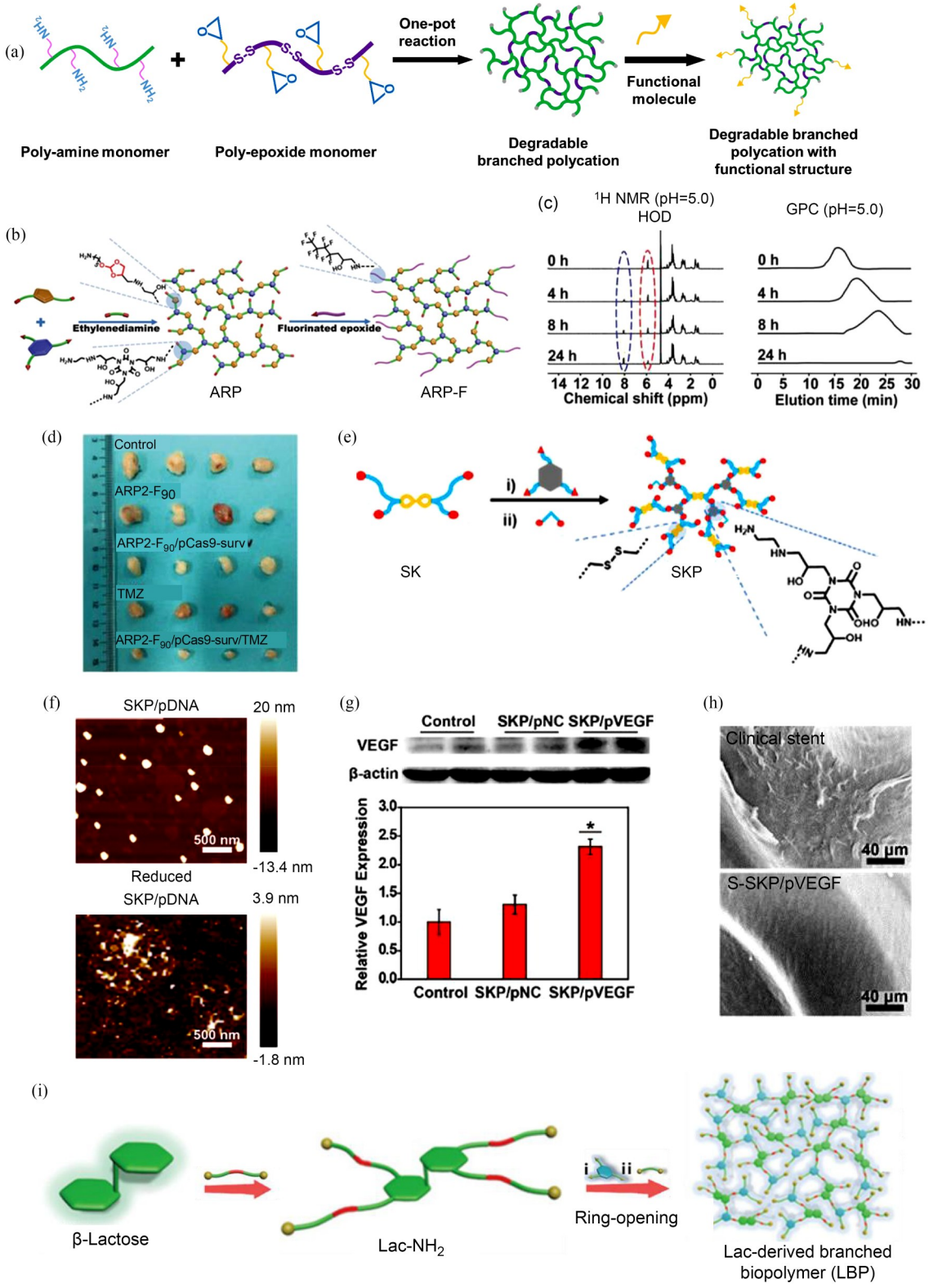

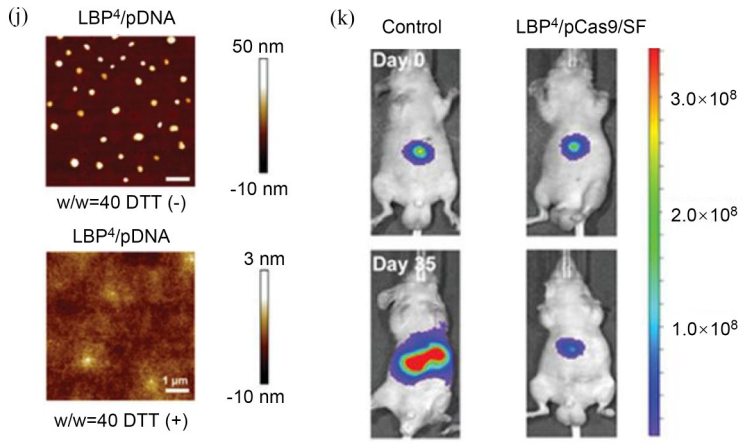

Fig. 1 (a) One-pot poly-amine and poly-epoxy ring-opening reaction for degradable branched polycation with functional structure. (b) Schematic illustration of the preparation of fluorinated acid-responsive polycation (ARP-F); (c) Degradation characterization of typical ARP2-F_{90}; (d) Images of A549 tumors after different treatments (Reprinted with permission from Ref.[36]; Copyright (2018) Wiley-VCH). (e) Schematic illustration of the preparation of SKP; (f) AFM images of typical SKP/pDNA complexes in neutral and reductive environments; (g) Western blot analysis of related VEGF protein expressions after 72 h transfection; (h) Representative SEM images of rabbit arterial segments treated with clinical stent and S-SKP/pVEGF at the fourth week after implantation (Reprinted with permission from Ref.[37]; Copyright (2019) American Chemical Society). (i) Schematic illustration of the preparation of lactose-derived branched biopolymer (LBP); (j) AFM images of LBP^4/pDNA complex at the mass ratio of 40 in the absence (−) and presence (+) of DTT; (k) Representative bioluminescence images of control and LBP^4/pCas9/SF treatment groups at 0th and 35th day (Reprinted with permission from Ref.[38]; Copyright (2019) Wiley-VCH).

诱导的Toll样受体激活、减少炎症细胞因子分泌、改善血液高凝状态，为治疗严重腹部创伤提供了一种新颖且前景广阔的治疗方案(图2(b)和2(c)). 在SS-HP的基础上，研究者通过对终端的修饰，赋予了SS-HP更多功能. Su等[40]通过开环反应为SS-HPT引入氟化烷基链，让递送载体更容易跨越生物屏障，从而提高转染效率. 研究者进一步设计并构建了多功能核酸递送系统SS-HPT-F108/pMIP-3β-KR，该核酸递送系统在有效进行光动力治疗的同时能最大程度地调动机体免疫行为，实现了光动力/免疫联合治疗，可有效抑制肿瘤的生长(图2(d)和2(e)). Wu[41]使用羰基二咪唑将维生素A(VA)上的羟基活化，与SS-HPT的胺基反应得到修饰上VA的SS-HPVA，并运载了pshRNA-TGFβ1基因沉默质粒用于肝纤维化治疗. 该核酸递送系统可靶向肝星状细胞，并被证明可以有效地逆转肝纤维化，并对各个器官均无毒副作用，具有良好的体内应用潜力(图2(f)和2(g)). Pan等[42]在合成SS-HPT后加入3-氨基苯硼酸继续反应，合成苯硼酸功能化的SS-HPT (SS-HPT-P). 研究者使用SS-HPT-P递送构建的治疗性质粒pNPMN-PBase，苯硼酸在可与肝脏中

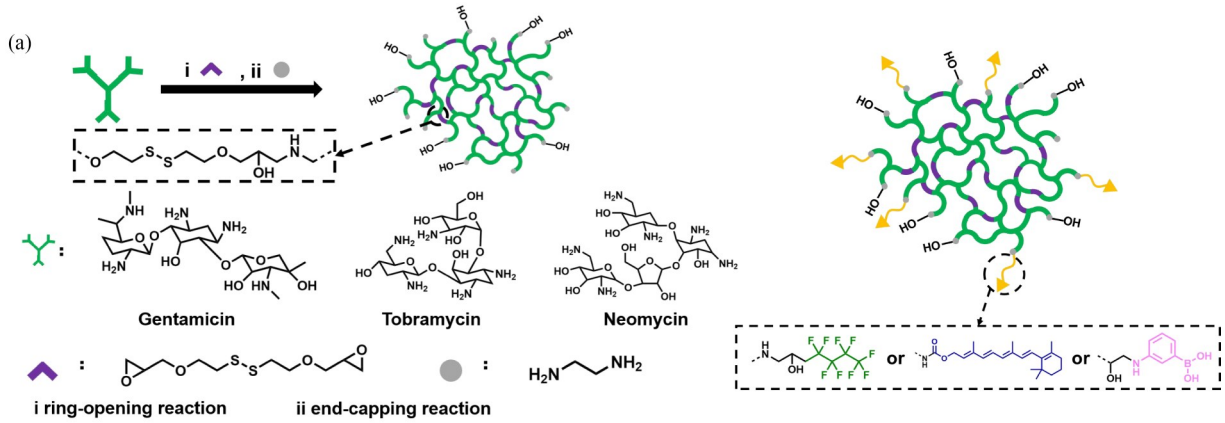

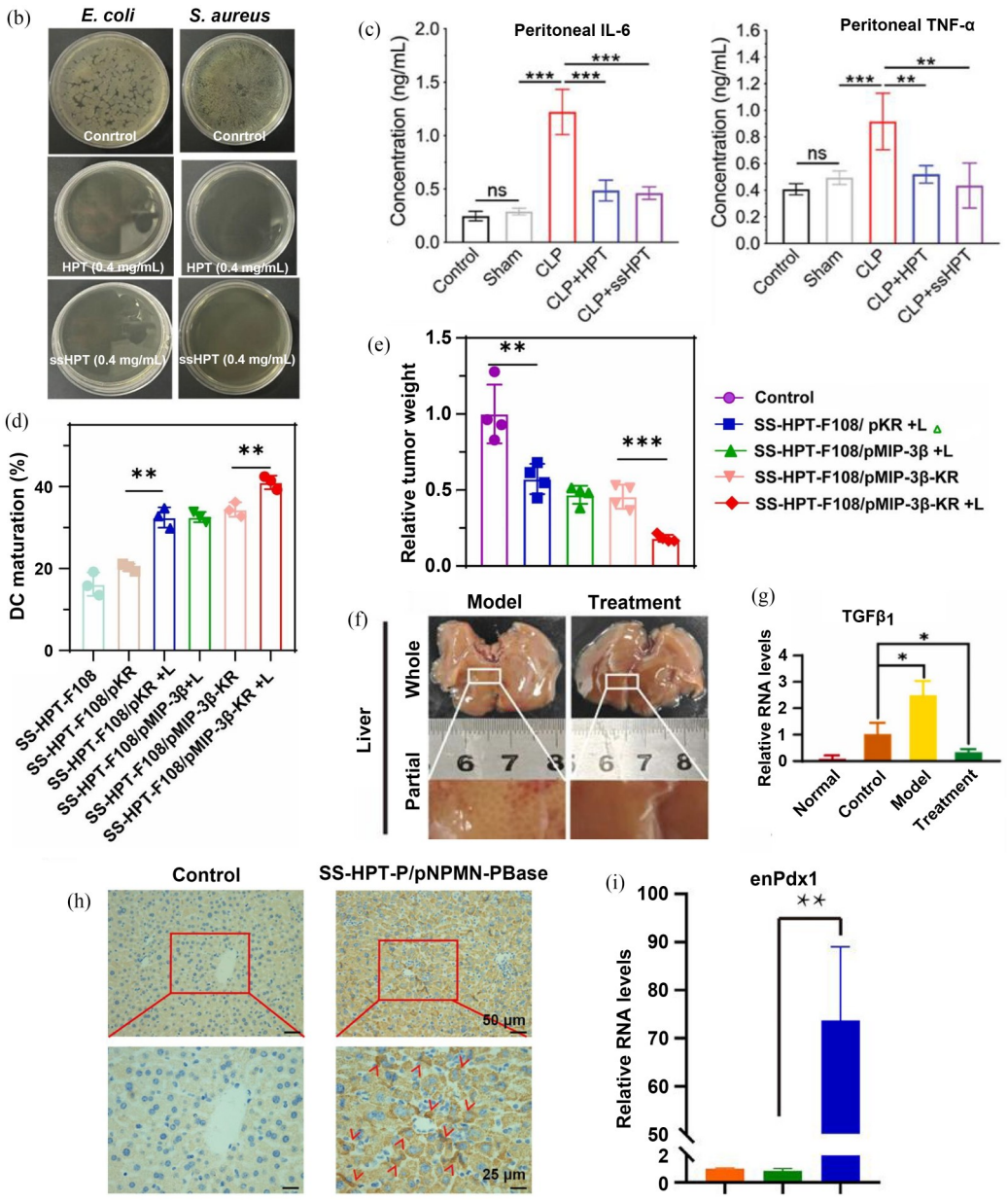

Fig. 2 (a) Schematic illustration for multifunctional aminoglycosides-based hyperbranched polymers with antibacterial activity, biocompatibility, and gene transfection capability and structure of functionalized SS-HPT. (b) Surface antibacterial activity of HPT and SS-HPT against *E. coli* and *S. aureus* after 24 h of incubation at 37 ℃; (c) The levels of IL-6 and TNF-α in peritoneal fluid were measured in different treatment groups at 24 h post-CLP (n=6, all data were presented as mean ±S.D.; $^{*}p$<0.05, $^{**}p$<0.01, $^{***}p$<0.001. Unpaired t-tests for two groups and ordinary one-way ANOVA with Tukey's Multiple Comparison test for three or more groups were used to analyze the differences between groups.) (Reprinted with permission from Ref.[39]; Copyright (2024) Wiley-VCH). (d) Quantification analysis of matured DCs ($CD80^{+}$ $CD86^{+}$ gated on $CD11c^{+}$ DCs) were incubated with culture mediums of 4T1 cells treated with different formulations after different treatments (n=3, data are mean ±S.D.; $^{**}p$< 0.01, $^{***}p$<0.001, $^{****}p$<0.0001. p values were determined using two-way analysis of variance with a student's t-test.); (e) Weights of excited tumors from primary sites at the end of antitumor study (n=4, date are mean ±S.D.; $^{*}p$<0.05, $^{**}p$<0.01, $^{***}p$<0.001. p values were determined using two-way analysis of variance with a student's t-test.) (Reprinted with permission from Ref.[40]; Copyright (2024) Elsevier BV). (f) Gross phenotypic pattern of liver captured by digital camera; (g) mRNA expression of liver fibrosis-related genes in liver (n=3, data were shown as mean ±S.D. deviation; $^{*}p$<0.05, $^{**}p$<0.01, $^{***}p$<0.001. Student's t-test was used to compare the differences between the two groups.) (Reprinted with permission from Ref.[41]; Copyright (2023) Elsevier). (h) Immumohistochemical staining of INSULIN in liver. A large amount of dark brown INSULIN staining was demonstrated in the liver of diabetic mice under SS-HPT-P/pNPMN-PBase treatment. There is almost no dark brown INSULIN staining in the liver of non-treated diabetic mice. The top row of each group was observed at 100 times magnification, and the bottom row of each group was observed at 200 times magnification; (i) The mRNA expression of insulin expression/secretion related genes (n=3, data were shown as mean ±S.D. deviation; $^{*}p$<0.05, $^{**}p$<0.01, $^{***}p$<0.001. Student's t-test was used to compare the differences between the two groups.) (Reprinted with permission from Ref.[42]; Copyright (2022) Elsevier).

过量表达的唾液酸形成稳定的硼酸酯从而靶向肝脏细胞，用于糖尿病的治疗. 研究表明，该递送系统能有效缓解糖尿病及其并发症的发生(图2(h)和2(i)).

2 NCA开环聚合构建策略

批量生产分子量可控、分子量分布窄的可降解阳离子聚合物有利于材料的应用，伯胺引发剂引发NCA单体的开环聚合被广泛认为是制备公斤级(以上)及高分子量聚氨基酸的最为有效的方法之一. 伯胺可与NCA单体中的5-CO发生亲核加成反应，随后NCA开环、质子转移，形成不稳定的氨基甲酸中间体，该中间体经过脱羧反应，释放出二氧化碳，生成新伯胺并作为反应中心维持聚合反应(图3(a)). 合成的聚氨基酸(聚肽)类材料因化学结构多样、有理想的生物降解性能、较低的细胞毒性而备受关注. 如图3(b)所示，Song等[43]通过由壳聚糖(CS)的伯胺基团、ED能化的环糊精(CD)或葡聚糖(Dex)引发的*β*-苄基-*L*-天冬氨酸*N*-羧酸酐(BLA-NCA)开环聚合，制备出不同类型多糖-PBLA接枝聚合物，随后与ED氨解，生成多种类型的多糖-PAsp接枝聚合物载体. 研究表明三种新载体具有有效的pDNA凝聚能力、良好的降解性和较低的细胞毒性(图3(c)和3(d)).

虽然NCA聚合可以批量生产可降解的聚肽类阳离子聚合物，然而这种聚合方法反应速度慢，通常需要2~3天的时间完成；同时，由于NCA单体稳定性一般较差，长时间反应可能导致副反应产生；最重要的是NCA聚合对水分高度敏感，部分单体甚至对氧气也十分敏感，聚合反应往往需要在手套箱内惰性气体保护下操作进行，反应条件严苛，极大地限制了聚肽材料的制备和应用研究. 解决这些核心问题是扩大NCA开环聚合应用的关键. 如图3(e)所示，Wu等[44]发现六甲基二硅基胺基锂(LiHMDS)作为引发剂可以使NCA环上3-NH去质子化，从而获得NCA负离子，引发聚合反应. LiHMDS引发的NCA开环聚合反应在几分钟到几小时即可完成，极大缩短了聚合反应时间；同时，首次实现了在普通环境条件下的NCA开环聚合，制备出具有可控二级结构、大分子量、窄分子量分布的聚肽(图3(f)). 此后，Wu等[45]又发现羧酸盐(四烷基铵羧酸盐)可稳定氨基甲酸根阴离子，并利用末端四烷基氨基甲酸铵作为反应中心，采用“协同加成和脱羧”机制进行链增长，实现NCA快速聚合(图3(g)和3(h)). 羧酸盐作为一类新的引发剂，即使在水相环境中使用未提纯NCA单体也可以实现超快速聚合，实现了NCA聚合引体系的突破.

NCA开环聚合制备的聚肽类阳离子聚合物主链上存在大量肽键，在人体内可在酶的作用下发生降解，生成无毒的多肽或氨基酸，且在保持了高度生物相容性、生物可降解性等特点的同时又具有高效的抗菌活性，因而在抗菌领域备受关注. 如图4(a)所示，Shi等[46]使用双(2-氨基丙基醚) 聚丙二醇引发*γ*-4-(3-氯丙氧羰基)苄基-*L*-谷氨酸基-*N*-羧酸酐进行开环聚合，然后经亲核取代将侧链上的Cl原子替换为叠氮基，最后通过1,3-偶极环加成将带正电荷的咪唑鎓环有效修饰在多肽骨架上，合成咪唑基嵌段共聚肽(PPG_n-PIL_m). PPG_n-PIL_m细胞毒性小，且能够在水溶液中形成阳离子胶束，表现出优异的抗菌活性(图4(b)). 如图4(c)所示，Zhang等[47]通过模拟维生素U的季锍盐结构，利用NCA开环反应合成了一系列星状季锍盐抗菌肽. 该季锍盐抗菌肽具有良好生物相容性的同时也具有优异的抗菌性能. 实验证明它可以通过调节侧链的阳离子化程度，实现对革兰氏阳性菌与革兰氏阴性菌的细菌种类选择性(图4(d)和4(e)). 如图4(f)和4(g)所示，Jiang等[48]模拟宿主防御肽,以三氟甲磺酸甲酯(MeOTf)为引发剂，引发2-(*N*-叔丁氧羰基-*γ*-氨基丙基)-2-噁唑啉($ProNH_{Boc}Ox$)进行NCA开环聚合后，对NH-Boc基团进行脱保护和胍基修饰，合成了一系列胍基功能化聚(2-噁唑啉)$PGOx_n$. 之后，研究人员[49]合成了不同间隔基、不同链长的胍基化聚噁唑啉，其中甲基间隔基、10 mer链长(mer代表单体单元数量)的聚噁唑啉分子$PGMeOx_{10}$表现出最佳的抗真菌选择性和优越的抗真菌活性，并在真菌脑膜炎模型中能有效降低脑部的真菌负荷，阻止真菌对脑实质的入侵(图4(h)和4(i)).

3 双硫交换反应构建策略

在温和的反应条件下实现聚合物的可控聚合可以精确控制聚合物结构、分子量和分散性，提高聚合物性能，是可降解阳离子聚合物递送活性生物大分子的必然要求. 动态键是一种新型的共

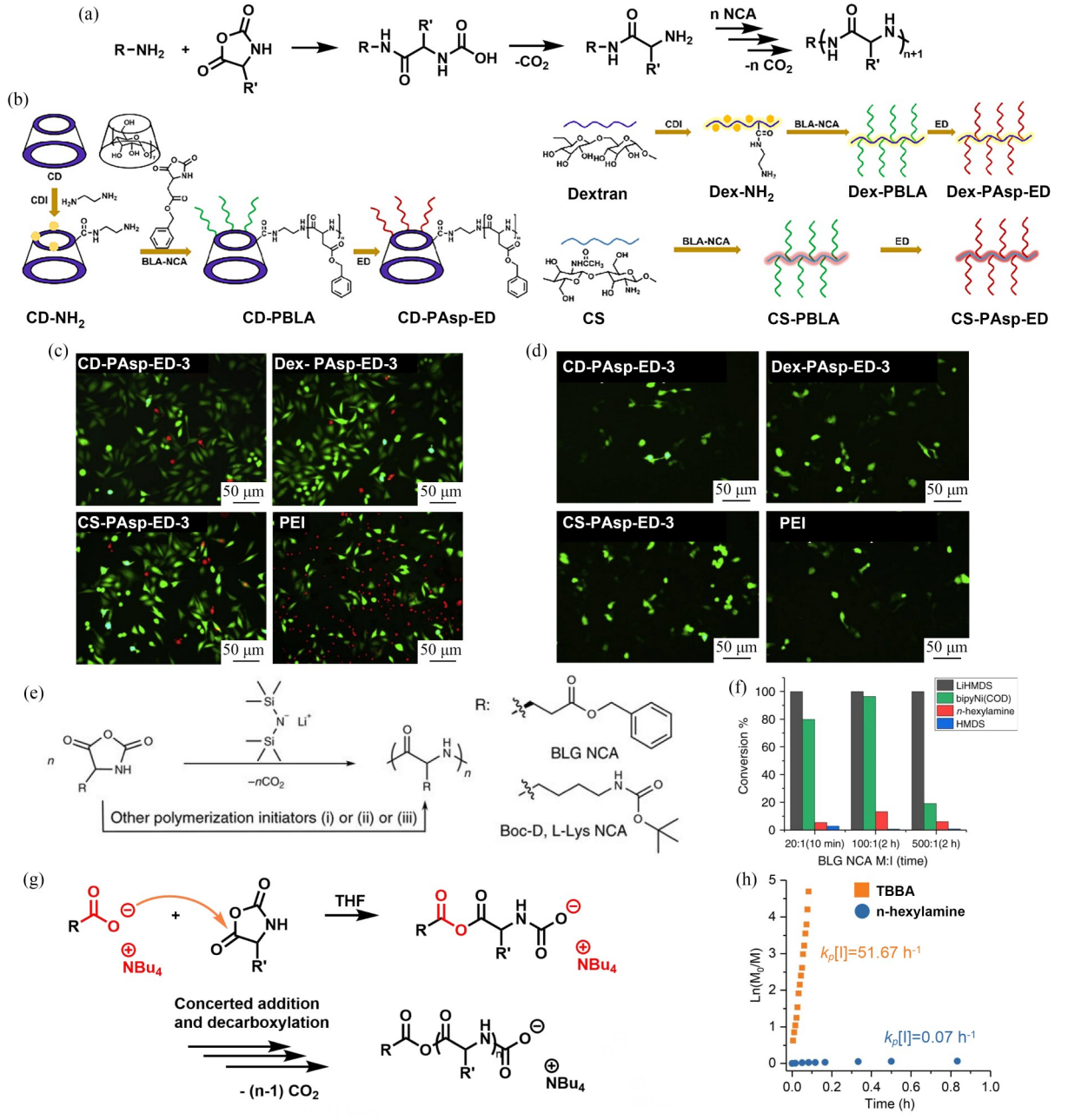

Fig. 3 (a) NCA ring-opening reaction polymerization mechanism diagram. (b) The preparation processes of degradable CD-PAsp-ED, Dex-PAsp-ED and CS-PAsp-ED; (c) FDA-PI staining HepG2 cells treated by CD-PAsp-ED-3, Dex-PAsp-ED-3, CS-PAsp-ED-3 and PEI at a N/P ratio of 20 (green: live; red: dead); (d) EGFP expression mediated by CD-PAsp-ED-3, Dex-PAsp-ED-3 and CS-PAsp-ED-3 at the optimal N/P ratio of 20 and PEI at the optimal N/P ratio of 10 in HepG2 cell lines. The percentages of the EGFP-positive HepG2 cells for CD-PAsp-ED-3, Dex-PAsp-ED-3 and CS-PAsp-ED-3 are 11%, 24% and 29%. PEI exhibited 17% of EGFP-positive HepG2 cells (Reprinted with permission from Ref.[43]; Copyright (2015) Elsevier BV). (e) NCA polymerization initiated by LiHMDS or other initiators in THF, initiator (i) *n*-hexylamine, initiator (ii) HMDS, initiator (iii) bipyNi(COD); (f) Conversion of BLG NCA in LiHMDS, *n*-hexylamine, HMDS or bipyNi(COD) initiated polymerization at variable NCA:initiator ratios using THF as the reaction solvent. The first column in each group represents the LiHMDS initiator group, the second represents the bipyNi(COD) initiator group, the third represents the n-hexylamine initiator group, and the fourth represents the HMDS initiator group (Reprinted with permission from Ref.[44]; Copyright (2018) Springer Nature). (g) Tetraalkylammonium carboxylate-initiated superfast NCA ROP; (h) Reaction rates for TBBA- and *n*-hexylamine-initiated polymerization of BLG NCA in THF at room temperature with M/I=100 and initial NCA concentration at 0.2 mol/L; k_p[I] reflex the rate of polymerization reaction, whereas k_p is the rate constant of the polymerization and [I] is the concentration of initiator (Reprinted with permission from Ref.[45]; Copyright (2021) Wiley-VCH).

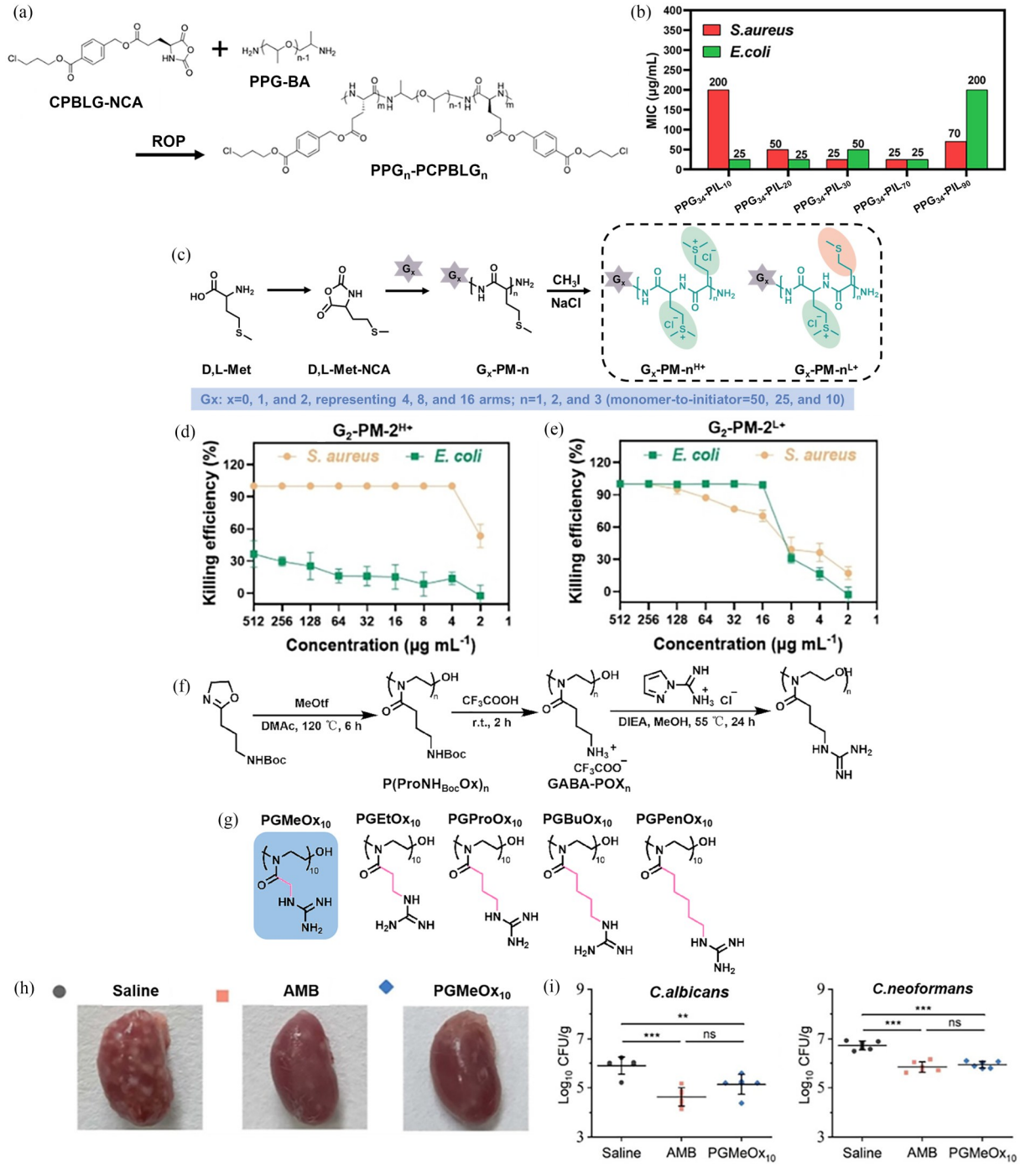

Fig. 4 (a) Ring-opening reaction routes of imidazolium-based block copolypeptides; (b) Plots of MIC vs imidazolium-based triblock copolymers. The first column in each group represents the result of *S. aureus* group, the second represents the result of the *E.coli* group (Reprinted with permission from Ref.[46]; Copyright (2021) American Chemical Society). (c) Synthetic route of G_x-PM-n^{H+} and G_x-PM-n^{L+} with tunable alkylation degree; (d) Antimicrobial efficiency of mixed bacteria treated by G_2-PM-2^{H+}; (e) Antimicrobial efficiency of mixed bacteria treated by G_2-PM-2^{L+} (Reprinted with permission from Ref.[47]; Copyright (2024) Wiley-VCH). (f) Synthetic scheme of guanidinium-rich poly(2-oxazoline)s ($PGOx_n$). *n* refers to the degree of polymerization (DP) of poly(2-oxazoline)s chain (Reprinted with permission from Ref.[48]; Copyright (2022) Wiley-VCH). (g) Structures of guanidinium-functionalized poly(2-oxazoline)s bearing different side chain spacer arms; (h) Representative images of saline-treated, AMB-treated, and $PGMeOx_{10}$-treated mouse kidneys that were infected by *C. albicans* K1; (i) Fungal burden of saline-treated, AMB-treated, and $PGMeOx_{10}$-treated mice brains that were infected by *C. albicans* K1 and *C. neoformans* H99 (n=6, all mean ±S.D. deviation was indicated by the error bars; $^{*}p<0.05$, $^{**}p<0.01$, $^{***}p<0.001$. Significance analyses between the two groups were performed using two-tailed student's t-test.). Each data point represents $\log_{10}$ (CFU/g) from one brain sample of one mouse (Reprinted with permission from Ref.[49]; Copyright (2023) American Chemical Society).

价化学键，不同于传统的共价键和离子键，其具有可逆性和可控性. 动态共价键可以在特定情况如光照、温度、pH或催化剂等条件下发生解离或缔合，整个过程处于动态平衡中. 在众多动态化学键中，二硫键是决定许多蛋白质动态特性的关键因素. 二硫键同时兼具稳健性和动态性的特点，可以在温和的条件下实现快速的硫醇-二硫化物交换反应且结构可控. 硫醇化合物上的巯基失去质子生成硫负离子(S^-)，S^-进攻环状二硫化物，使得原有的—S—S—断裂，生成新的—S—S—分子，并产生一个新的S^-活性位点，继续进攻环状二硫化物，实现聚合. 生成的聚二硫化物在还原剂的作用下，—S—S—可以发生断裂，还原成巯基，从而实现降解(图5(a)). 调节反应时间、缓冲液/*N*,*N*-二甲基甲酰胺(DMF)比例、改变亲核试剂浓度、缓冲溶液的pH值等条件，可以制备出一系列聚合度和分子量可控的可降解阳离子聚合物. Zhu等[50]以氧基聚乙二醇硫醇为引发剂，引发胍基基团改性的硫辛酸进行双硫交换反应，制备了一系列聚合度可控的可降解聚胍化合物$mPEG_{225}$-*b*-PSS_n (图5(b)). Yu等[51]以具有7个巯基位点的环糊精为引发剂，引发二硫单体进行双硫交换反应，制备了一系列聚合度可控的可降解阳离子聚合物基因载体*β*-CD-*g*-PSS_n (图5(c)). Mu等[52]通过葡聚糖-硫醇(Dex-SH)和硫辛酸衍生物的双硫交换反应，制备了一系列阳离子多糖偶联物(Dex-*g*-PSS_n) (图5(d)).

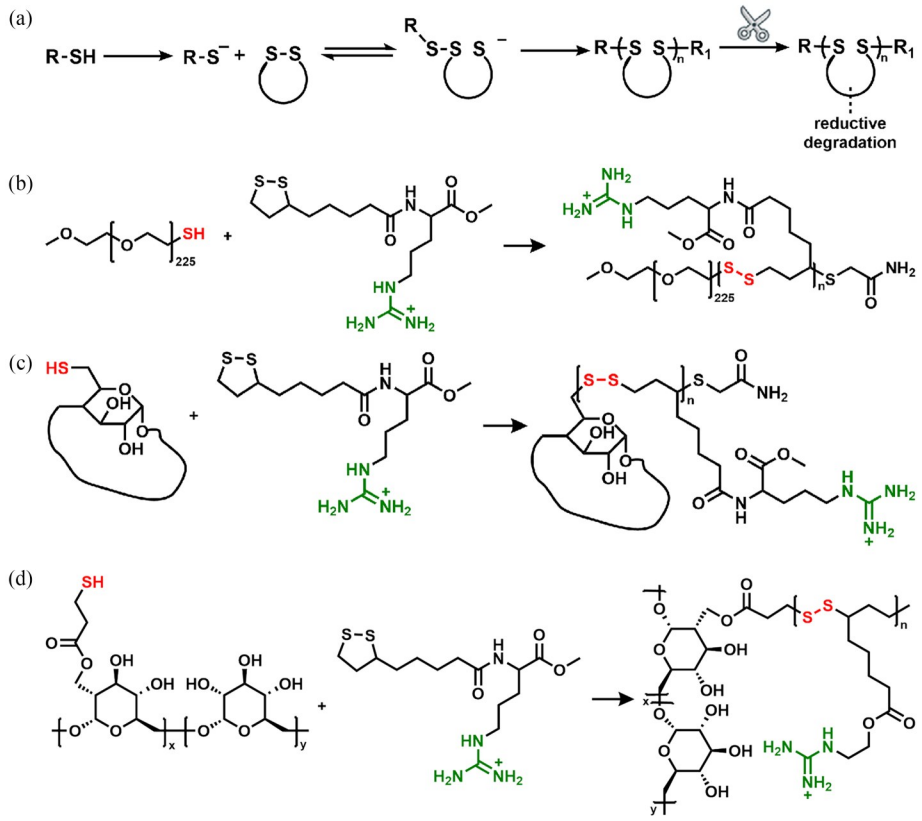

Fig. 5 (a) Mechanism diagram of bisulfide exchange reaction and reductive degradation of disulfide polymers. (b) Build strategy for PEG_{225}-*b*-PSS_n (Reprinted with permission from Ref.[50]; Copyright (2022) Wiley-VCH). (c) Build strategy for *β*-CD-*g*-PSS_n (Reprinted with permission from Ref.[51]; Copyright (2023) Wiley-VCH). (d) Build strategy for Dex-*g*-PSS_n (Reprinted with permission from Ref.[52]; Copyright (2022) Wiley-VCH).

双硫交换反应制备方法简单、条件温和，生成的聚二硫化物易于修饰，二硫键可以在还原性物质(如谷胱甘肽)的作用下发生响应性断裂，促进所包裹药物的释放，且大大降低了材料的毒性，被广泛用于生物大分子药物载体. Zhu等[50]制备的聚胍化合物$mPEG_{225}$-*b*-PSS_{26}有效递送质粒DNA (pKR-p53和pEGF)，并在还原性物质的作用下实现有效的降解，释放pDNA实现光动力和基因联合抗肿瘤治疗和针对表皮全层缺损的抗菌促愈合(图6(a)和6(b)). Yu等[51]合成的*β*-CD-*g*-

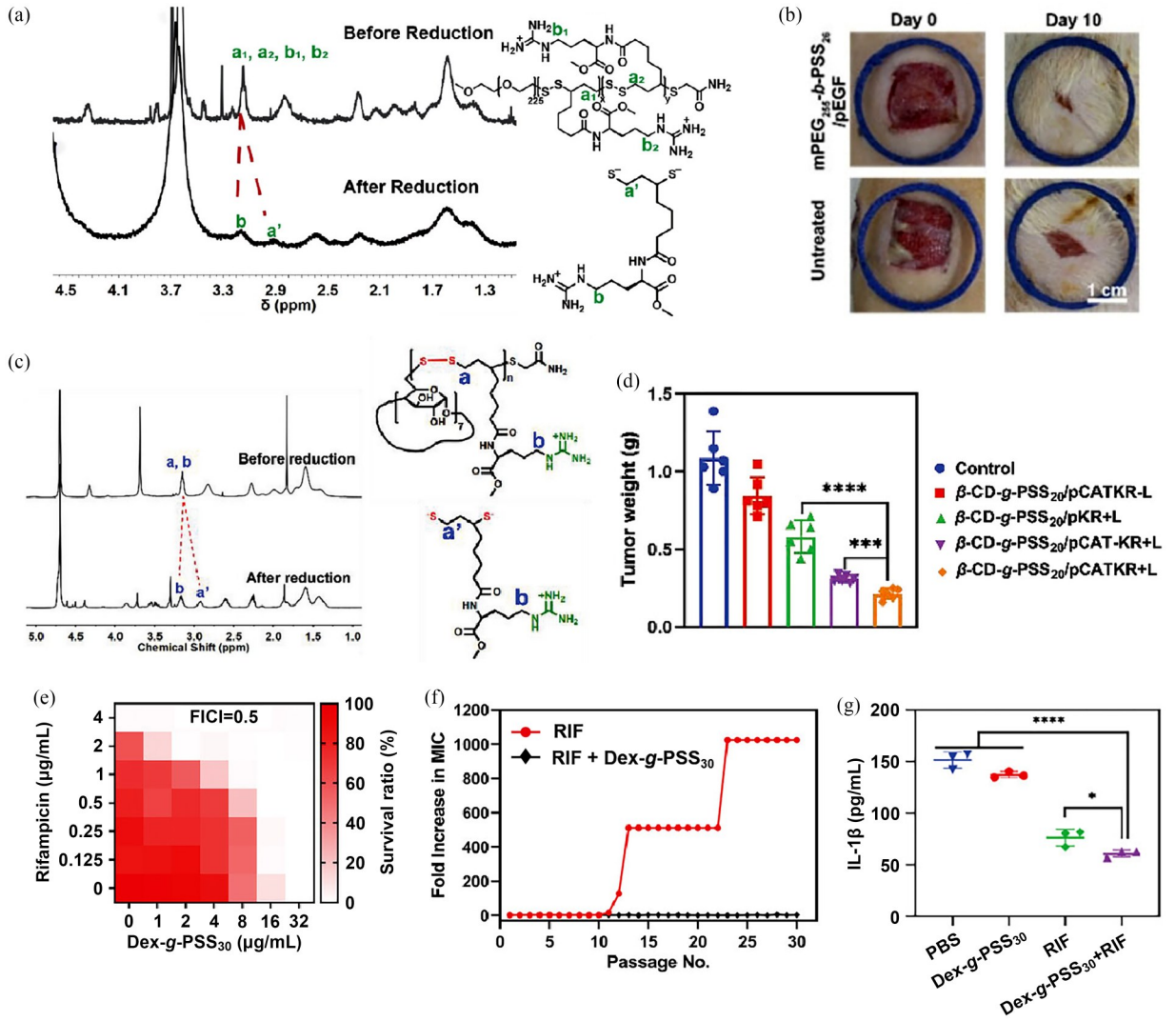

Fig. 6 (a) Typical ^{1}H-NMR (400 MHz) spectra of mPEG$_{225}$-*b*-PSS$_n$ before and after reduction; (b) Photographs of wound healing in the rat model on Day 0 and Day 10 (Reprinted with permission from Ref.[50]; Copyright (2022) Wiley-VCH). (c) Typical ^{1}H-NMR (400 MHz) spectra of *β*-CD-*g*-PSS$_{20}$ before and after reduction; (d) SCC-7 tumor weights after different treatments. Scale bar=50 μm (n=6, data are presented as the mean ±S.D. deviation; *p<0.05, **p<0.01, ***p<0.001, and ****p<0.0001. p values were determined using a one-way analysis of variance with a student's t-test). (Reprinted with permission from Ref.[51]; Copyright (2023) Wiley-VCH). (e) Synergism between rifampicin (RIF) and Dex-*g*-PSS$_{30}$ was evaluated against MDR-AB cells using the fractional inhibitory concentration (FIC) index; (f) Dex-*g*-PSS$_{30}$ (8 μg/mL) addition prevents rifampicin (RIF) resistance in MDR-AB cells; (g) Statistical analysis of inflammatory cells after different treatments (n=3, data are shown as the mean ±S.D. deviation; *p<0.05, **p<0.01, ***p<0.001, and ****p<0.0001. Statistical significance was calculated using the two-tailed Student's t-test). (Reprinted with permission from Ref.[52]; Copyright (2022) Wiley-VCH).

PSS$_{20}$载体可以有效递送过氧化氢酶和红色荧光蛋白KillerRed的融合质粒(pCATKR)，并有效表达融合蛋白CATKR，该融合蛋白提高了级联催化治疗的催化效率，产生了更多的活性氧，显示出在肿瘤乏氧条件下更好的肿瘤治疗效果(图6(c)和6(d)). Mu等[52]通过简单、温和、可控的双硫交换聚合，制备的可降解阳离子多糖共轭化合物Dex-*g*-PSS$_{30}$可以通过多种方法降低多重耐药鲍曼不动杆菌(MDR-AB)对抗生素的耐药性，从而增加抗生素利福平(RIF)在MDR-AB内部的积累；此外Dex-*g*-PSS$_{30}$生物响应降解，提高生物安全性(图6(e)~6(g)).

4　总结与展望

本文介绍了3种构建高性能可降解阳离子聚

合物的制备策略，包括“一锅法”多胺基-多环氧开环聚合、NCA开环聚合和双硫交换聚合. “一锅法”多胺基-多环氧开环聚合反应仅需一步即可完成，其制备方法简便，分子设计灵活；NCA开环聚合反应在保证材料降解性能的同时，可以进一步实现对分子量的控制；双硫交换聚合反应可在温和的条件下实现可控聚合，并能够在还原性的病灶部位进行响应，按需释放药物. 本文旨在启发研究人员灵活选择制备方式，设计和开发具有可降解的高性能阳离子聚合物，以满足生物医学的不同需求.

高性能可降解阳离子聚合物仍有很大的发展空间，例如可以开发多组分聚二硫化物、掺入协同官能团拓展实现聚二硫化物的多功能应用、提高聚二硫化物对还原环境的敏感性等. 此外，虽然大量性能优异的可降解阳离子聚合物不断被报道，然而高性能可降解阳离子聚合物的生物应用大都停留在基础研究层面，距离临床上的应用仍存在一定差距. 总之，可降解高性能阳离子聚合物材料的优势非常明显，具有非常广阔的前景和市场，相信随着技术的不断进步和创新，可降解高性能阳离子聚合将带来更多的惊喜和突破.

作者简介：俞丙然，男，1983年生. 北京化工大学材料科学与工程学院教授，博士生导师. 2006年、2010年、2013年于兰州大学分别获学士、硕士、博士学位. 2014年加入北京化工大学材料科学与工程学院. 在基于药物、基因控释生物材料以及抗菌抗感染生物医用材料等方面开展了广泛的研究，目前在*J. Am. Chem. Soc.*，*Adv. Mater.*，*Biomaterials*等国际期刊上发表论文60余篇. 2021年获批国家自然基金优秀青年基金，并主持国家自然基金面上项目2项，青年基金项目1项. 参与国家自然基金重点项目1项，重点研发计划1项.

作者简介：徐福建，男，1976年生. 北京化工大学材料科学与工程学院院长，生物医用材料北京实验室执行主任，天然高分子医用材料教育部重点实验室主任，博士生导师. 1999年于华东理工大学获学士学位，2002年于中国科学院过程工程研究所获硕士学历，2006年于新加坡国立大学获博士学位. 2013年获国家杰出青年科学基金资助；2014年入选“长江学者奖励计划”特聘教授；2018年入选北京高校卓越青年科学家计划；担任*Biomater. Sci.*副主编，*Mater. Today Bio.*，*Chinese J. Polym. Sci.*，*Sci. China Chem.*及《中国科学：化学》编委. 主要从事医用高分子材料应用基础研究，在药物控释载体、抗菌材料以及多糖功能化方面开展了广泛应用基础研究. 在*Chem. Rev.*，*Nat. Commun.*，*Adv. Mater.*等期刊发表论文250余篇，他引8000余次，申请/授权发明专利60余项.

REFERENCES

1 Casper, J.; Schenk, S. H.; Parhizkar, E.; Detampel, P.; Dehshahri, A.; Huwyler, J. Polyethylenimine (PEI) in gene therapy: current status and clinical applications. *J. Control. Release*, **2023**, 362, 667−691.

2 Fattahi, N.; Gorgannezhad, L.; Masoule, S. F.; Babanejad, N.; Ramazani, A.; Raoufi, M.; Sharifikolouei, E.; Foroumadi, A.; Khoobi, M. PEI-based functional materials: fabrication techniques, properties, and biomedical applications. *Adv. Colloid Interface Sci.*, **2024**, 325, 103119.

3 Li, J. C.; Yu, X. R.; Shi, X. Y.; Shen, M. W. Cancer nanomedicine based on polyethylenimine-mediated multifunctional nanosystems. *Prog. Mater. Sci.*, **2022**, 124, 100871.

4 Dai, Y.; Zhang, X. J. Cationic polycarbonates *via* ring-opening polymerization: design, synthesis, and applications. *Polym. Chem.*, **2019**, 10(3), 296−305.

5 Tempelaar, S.; Mespouille, L.; Coulembier, O.; Dubois, P.; Dove, A. P. Synthesis and post-polymerisation modifications of aliphatic poly(carbonate)s prepared by ring-opening polymerisation. *Chem. Soc. Rev.*, **2013**, 42(3), 1312−1336.

6 Yu, W.; Maynard, E.; Chiaradia, V.; Arno, M. C.; Dove, A. P. Aliphatic polycarbonates from cyclic carbonate monomers and their application as biomaterials. *Chem. Rev.*, **2021**, 121(18), 10865−10907.

7 Yin, M. L.; Wan, S. S.; Ren, X. H.; Chu, C. C. Development of inherently antibacterial, biodegradable, and biologically active chitosan/pseudo-protein hybrid hydrogels as biofunctional wound dressings. *ACS Appl. Mater. Interfaces*, **2021**, 13(12), 14688−14699.

8 Huang, Y. J.; Hu, H.; Li, R. Q.; Yu, B. R.; Xu, F. J. Versatile types of MRI-visible cationic nanoparticles involving pullulan polysaccharides for multifunctional gene carriers. *ACS Appl. Mater. Interfaces*, **2016**, 8(6), 3919−3927.

9 Wang, L. S.; Duan, L.; Liu, G.; Sun, J. F.; Shahbazi, M. A.; Kundu, S. C.; Reis, R. L.; Xiao, B.; Yang, X. Bioinspired polyacrylic acid-based dressing: wet adhesive, self-healing, and multi-biofunctional coacervate hydrogel accelerates wound healing. *Adv. Sci.*, **2023**, 10(16), 2207352.

10 Wu, Q. M.; Hu, Y.; Yu, B.; Hu, H.; Xu, F. J. Polysaccharide-based tumor microenvironment-responsive drug delivery systems for cancer therapy. *J. Control. Release*, **2023**, 362, 19−43.

11 van Bruggen, C.; Hexum, J. K.; Tan, Z.; Dalal, R. J.; Reineke, T. M. Nonviral gene delivery with cationic glycopolymers. *Acc. Chem. Res.*, **2019**, 52(5), 1347−1358.

12 Jin, M.; Liu, B. H.; Zhang, Z.; Mu, Y. L.; Ma, L.; Yao, H.; Wang, D. A. Catechin-functionalized cationic lipopolymer based multicomponent nanomicelles for lung-targeting delivery. *Adv. Mater.*, **2024**, 36(17), 2302985.

13 Hu, Y. Z.; Nie, W.; Lyu, L.; Zhang, X. F.; Wang, W. Y.; Zhang, Y. C.; He, S.; Guo, A. J.; Liu, F.; Wang, B. L.; Qian, Z. Y.; Gao, X. Tumor-microenvironment-activatable nanoparticle mediating immunogene therapy and M2 macrophage-targeted inhibitor for synergistic cancer immunotherapy. *ACS Nano*, **2024**, 18(4), 3295−3312.

14 Schneider, P.; Zhang, H. Y.; Simic, L.; Dai, Z. Q.; Schrörs, B.; Akilli-Öztürk, Ö.; Lin, J.; Durak, F.; Schunke, J.; Bolduan, V.; Bogaert, B.; Schwiertz, D.; Schäfer, G.; Bros, M.; Grabbe, S.; Schattenberg, J. M.; Raemdonck, K.; Koynov, K.; Diken, M.; Kaps, L.; Barz, M. Multicompartment polyion complex micelles based on triblock polypept(o)ides mediate efficient siRNA delivery to cancer-associated fibroblasts for antistromal therapy of hepatocellular carcinoma. *Adv. Mater.*, **2024**, 36(41), 2404784.

15 陈华, 崔力允, 李圆凤, 刘勇, 马如江, 史林启. 苯硼酸功能化聚合物纳米载体用于蛋白质药物胞内递送. 高分子学报, **2023**, 54(4), 451−466.

16 Wong, K. H.; Guo, Z. P.; Jiang, D.; Zhou, X. Z.; Lin, L. Z.; Zhao, D. G.; Chen, M. W. Linear-like polypeptide-based micelle with pH-sensitive detachable PEG to deliver dimeric camptothecin for cancer therapy. *Asian J. Pharm. Sci.*, **2023**, 18(1), 100773.

17 Qian, Y. P.; Sun, Y. J.; Zhang, L. D.; Zhu, Y. W.; Li, N. Y.; Dong, F.; Xu, C.; An, N.; Chen, H.; Sun, Y. C.; Yu, B. R.; Wang, Y. G.; Xu, F. J. Oxygen-free polycationic photosensitizers for treatment of periodontal inflammation. *Adv. Funct. Mater.*, **2024**, 34(7), 2310636.

18 周睿毅, 佘蕴芮, 武月铭, 张君宇, 王靖, 刘润辉. 促内皮化β-多肽聚合物修饰的聚氨酯表面抗菌功能研究. 高分子学报, **2023**, 54(7), 1055−1063.

19 Feng, Y.; Guo, Z.; Chen, J.; Zhang, S.; Wu, J.; Tian, H.; Chen, X. Cationic polymer synergizing with a disulfide-containing enhancer achieved efficient nucleic acid and protein delivery. *Biomater. Sci.*, **2022**, 10(21), 6230−6243.

20 刘畅, 陈宇欣, 王江帆, 罗萱, 黄宇迪, 徐瑾蕾, 鄢国平, 陈思, 张先正. 基于枝化多肽的多功能药物递送系统用于肿瘤细胞核的精准靶向治疗. 高分子学报, **2018**, 49(6), 682−691.

21 范玲玲, 黎槟瑞, 张浩伟, 方艳. 表面抗菌功能涂层的构建及在生物医用材料中的应用研究. 高分子学报, **2021**, 52(3), 253−271.

22 Khodadadi Yazdi, M.; Zarrintaj, P.; Saeb, M. R.; Mozafari, M.; Bencherif, S. A. Progress in ATRP-derived materials for biomedical applications. *Prog. Mater. Sci.*, **2024**, 143, 101248.

23 Ahmed, M.; Narain, R. Progress of RAFT based polymers in gene delivery. *Prog. Polym. Sci.*, **2013**, 38(5), 767−790.

24 Mather, B. D.; Viswanathan, K.; Miller, K. M.; Long, T. E. Michael addition reactions in macromolecular design for emerging technologies. *Prog. Polym. Sci.*, **2006**, 31(5), 487−531.

25 Pesenti, T.; Nicolas, J. 100th Anniversary of macromolecular science viewpoint: degradable polymers from radical ring-opening polymerization: latest advances, new directions, and ongoing challenges. *ACS Macro Lett.*, **2020**, 9(12), 1812−1835.

26 Huang, Y. J.; Ding, X. K.; Qi, Y.; Yu, B. R.; Xu, F. J. Reduction-responsive multifunctional hyperbranched polyaminoglycosides with excellent antibacterial activity, biocompatibility and gene transfection capability. *Biomaterials*, **2016**, 106, 134−143.

27 Song, Z. Y.; Han, Z. Y.; Lv, S. X.; Chen, C. Y.; Chen, L.; Yin, L. C.; Cheng, J. J. Synthetic polypeptides: from polymer design to supramolecular assembly and biomedical application. *Chem. Soc. Rev.*, **2017**, 46(21), 6570−6599.

28 Tao, X. F.; Li, M. H.; Ling, J. *α*-Amino acid *N*-thiocarboxyanhydrides: a novel synthetic approach toward poly(*α*-amino acid)s. *Eur. Polym. J.*, **2018**, 109, 26−42.

29 Feng, H.; Fabrizi, J.; Li, J.; Mayer, C. Syntheses of polypeptides and their biomedical application for anti-tumor drug delivery. *Int. J. Mol. Sci.*, **2022**, 23(9), 5042.

30 Zhang, Q.; Qu, D. H.; Feringa, B. L.; Tian, H. Disulfide-mediated reversible polymerization toward intrinsically dynamic smart materials. *J. Am. Chem. Soc.*, **2022**, 144(5), 2022−2033.

31 Zheng, B.; Bai, T.; Tao, X.; Ling, J. An inspection into multifarious ways to synthesize poly(amino acid)s. *Macromol. Rapid Commun.*, **2021**, 42(22), e2100453.

32 王元琛, 王俊凯, 俞丙然, 徐福建. 基于胺基与环氧的开环反应构建医用阳离子聚合物. 高分子学报, **2022**, 53(7), 828−841

33 Duan, S.; Yu, B.; Gao, C.; Yuan, W.; Ma, J.; Xu, F. J. A facile strategy to prepare hyperbranched hydroxyl-rich polycations for effective gene therapy. *ACS Appl. Mater. Interfaces*, **2016**, 8(43), 29334−29342.

34 Mou, Q. B.; Ma, Y.; Jin, X.; Zhu, X. Y. Designing hyperbranched polymers for gene delivery. *Mol. Syst. Des. Eng.*, **2016**, 1(1), 25−39.

35 Su, M. R.; Hu, Z. C.; Sun, Y. J.; Qi, Y.; Yu, B. R.; Xu, F. J. Hydroxyl-rich branched polycations for nucleic acid delivery. *Biomater. Sci.*, **2024**, 12(3), 581−595.

36 Qi, Y.; Song, H.; Xiao, H.; Cheng, G.; Yu, B.; Xu, F. J. Fluorinated acid-labile branched hydroxyl-rich nanosystems for flexible and robust delivery of plasmids. *Small*, **2018**, 14(42), e1803061.

37 Ye, W. J.; Chen, Y. M.; Tang, W. X.; Zhang, N.; Li, Z. H.; Liu, Z. J.; Yu, B. R.; Xu, F. J. Reduction-responsive nucleic acid delivery systems to prevent in-stent restenosis in rabbits. *ACS Appl. Mater. Interfaces*, **2019**, 11(31), 28307−28316.

38 Qi, Y.; Liu, Y.; Yu, B.; Hu, Y.; Zhang, N.; Zheng, Y.; Yang, M.; Xu, F. J. A lactose-derived CRISPR/Cas9 delivery system for efficient genome editing *in vivo* to treat orthotopic hepatocellular carcinoma. *Adv. Sci.*, **2020**, 7(17), 2001424.

39 Xiao, Y.; Fang, H.; Zhu, Y.; Zhou, J.; Dai, Z.; Wang, H.; Xia, Z.; Tu, Z.; Leong, K. W. Multifunctional cationic hyperbranched polyaminoglycosides that target multiple mediators for severe abdominal trauma management. *Adv. Sci.*, **2024**, 11(1), e2305273.

40 Su, M. R.; Wang, J. K.; Zhao, N. N.; Yu, B. R.; Wang, Y. G.; Xu, F. J. Genetically light-enhanced immunotherapy mediated by a fluorinated reduction-sensitive delivery system. *Biomaterials*, **2024**, 305, 122433.

41 Wu, T.; Qi, Y.; Xu, C.; Sui, D. D.; Xu, F. J. HSC-targeted delivery of shRNA-Tgf*β*1 by vitamin A-functionalized polyaminoglycoside for hepatic fibrosis therapy. *Nano Today*, **2023**, 50, 101887.

42 Pan, Y. Q.; Shao, M. Y.; Li, P.; Xu, C.; Nie, J. J.; Zhang, K.; Wu, S.; Sui, D. D.; Xu, F. J. Polyaminoglycoside-mediated cell reprogramming system for the treatment of diabetes mellitus. *J. Control. Release*, **2022**, 343, 420−433.

43 Song, H. Q.; Dou, X. B.; Li, R. Q.; Yu, B. R.; Zhao, N. N.; Xu, F. J. A general strategy to prepare different types of polysaccharide-graft-poly(aspartic acid) as degradable gene carriers. *Acta Biomater.*, **2015**, 12, 156−165.

44 Wu, Y. M.; Zhang, D. F.; Ma, P. C.; Zhou, R. Y.; Hua, L.; Liu, R. H. Lithium hexamethyldisilazide initiated superfast ring opening polymerization of alpha-amino acid N-carboxyanhydrides. *Nat. Commun.*, **2018**, 9, 5297.

45 Wu, Y. M.; Chen, K.; Wu, X.; Liu, L. Q.; Zhang, W. W.; Ding, Y.; Liu, S. Q.; Zhou, M.; Shao, N.; Ji, Z. M.; Chen, J. C.; Zhu, M. H.; Liu, R. H. Superfast and water-insensitive polymerization on *α*-amino acid *N*-carboxyanhydrides to prepare polypeptides using tetraalkylammonium carboxylate as the initiator. *Angew. Chem. Int. Ed.*, **2021**, 60(50), 26063−26071.

46 Shi, Z.; Zhang, X.; Yu, Z.; Yang, F.; Liu, H.; Xue, R.; Luan, S.; Tang, H. Facile synthesis of imidazolium-based block copolypeptides with excellent antimicrobial activity. *Biomacromolecules*, **2021**, 22(6), 2373−2381.

47 Zhang, Z. Y.; Wang, X. D.; Liu, J. Y.; Yang, H. W.; Tang, H. Y.; Li, J.; Luan, S. F.; Yin, J. H.; Wang, L.; Shi, H. C. Structural element of vitamin U-mimicking antibacterial polypeptide with ultrahigh selectivity for effectively treating MRSA infections. *Angew. Chem. Int. Ed.*, **2024**, 63(7), e202318011.

48 Jiang, W. N.; Zhou, M.; Cong, Z. H.; Xie, J. Y.; Zhang, W. J.; Chen, S.; Zou, J. C.; Ji, Z. M.; Shao, N.; Chen, X.; Li, M. Q.; Liu, R. H. Short guanidinium-functionalized poly(2-oxazoline)s displaying potent therapeutic efficacy on drug-resistant fungal infections. *Angew. Chem. Int. Ed.*, **2022**, 61(17), e202200778.

49 Jiang, W. N.; Zhou, M.; Chen, S.; Xie, J. Y.; Chen, M. Z.; Zhang, H. D.; Wu, Y. M.; Chen, X.; Liu, R. H. Peptide-mimicking poly(2-oxazoline)s possessing potent antifungal activity and BBB penetrating property to treat invasive infections and meningitis. *J. Am. Chem. Soc.*, **2023**, 145(47), 25753−25765.

50 Zhu, Y. W.; Lin, M. Y.; Hu, W. T.; Wang, J. K.; Zhang, Z. G.; Zhang, K.; Yu, B. R.; Xu, F. J. Controllable disulfide exchange polymerization of polyguanidine for effective biomedical applications by thiol-mediated uptake. *Angew. Chem. Int. Ed.*, **2022**, 61(23), e202200535.

51 Yu, D.; Wang, Y. C.; Qu, S.; Zhang, N.; Nie, K. L.; Wang, J. K.; Huang, Y. C.; Sui, D. D.; Yu, B. R.; Qin, M.; Xu, F. J. Controllable star cationic poly(disulfide)s achieve genetically cascade catalytic therapy by delivering bifunctional fusion plasmids. *Adv. Mater.*, **2023**, 35(52), 2307190.

52 Mu, S. W.; Zhu, Y. W.; Wang, Y.; Qu, S.; Huang, Y. C.; Zheng, L.; Duan, S.; Yu, B. R.; Qin, M.; Xu, F. J. Cationic polysaccharide conjugates as antibiotic adjuvants resensitize multidrug-resistant bacteria and prevent resistance. *Adv. Mater.*, **2022**, 34(41), 2204065.

Review

High-performance Degradable Cationic Polymers Based on Ring-opening Reactions and Their Biological Applications

Ya-qi Zhao, Yu-jie Sun, Bing-ran Yu*, Fu-jian Xu*

(*College of Material Science and Engineering, Beijing University of Chemical Technology, Beijing 100029*)

Abstract Non-degradable cationic polymers can accumulate in the body, which can cause potential harm to human health and limit the application of cationic polymers. Therefore, it is important to develop cationic polymer materials with high biocompatibility and good degradability. Ring-opening reaction is one of the methods to obtain degradable cationic polymers with better degradability and biosafety. In this review, three

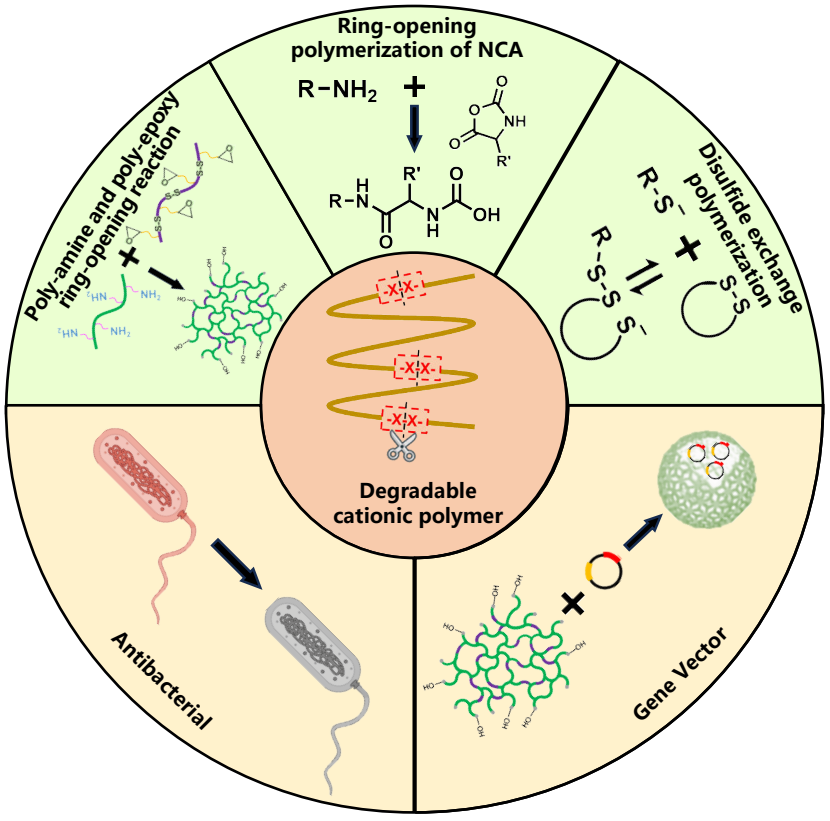

* Corresponding authors: Bing-ran Yu, E-mail: yubr@mail.buct.edu.cn
Fu-jian Xu, E-mail: xufj@mail.buct.edu.cn

strategies for the construction of degradable cationic polymers based on ring-opening reactions are presented, including the one-pot poly-amine and poly-epoxy ring-opening reaction, the ring-opening polymerization of *N*-carboxyanhydride (NCA), and the bisulfide-exchange reaction. The degradable cationic polymers with unique structures were prepared by the different construction strategies, including branched cationic polymers, peptide cationic polymers, and polydisulfides. Different structures endowed the degradable cationic polymers with higher performance. In addition, the biological applications of high performance degradable cationic polymers in nucleic acid delivery and antibacterial applications are summarized in this review.

Keywords Cationic polymers, Ring-opening reaction, Degradable, Nucleic acid delivery vector, Antibacterial materials